JPE 18-1-12

https://doi.org/10.6113/JPE.2018.18.1.129
ISSN(Print): 1598-2092 / ISSN(Online): 2093-4718

State-of-charge Estimation for Lithium-ion Battery using a Combined Method

Guidan Li†, Kai Peng*, and Bin Li*

†,*School of Electrical and Information Engineering, Tianjin University, Tianjin, China

Abstract

An accurate state-of-charge (SOC) estimation ensures the reliable and efficient operation of a lithium-ion battery management system. On the basis of a combined electrochemical model, this study adopts the forgetting factor least squares algorithm to identify battery parameters and eliminate the influence of test conditions. Then, it implements online SOC estimation with high accuracy and low run time by utilizing the low computational complexity of the unscented Kalman filter (UKF) and the rapid convergence of a particle filter (PF). The PF algorithm is adopted to decrease convergence time when the initial error is large; otherwise, the UKF algorithm is used to approximate the actual SOC with low computational complexity. The effect of the number of sampling particles in the PF is also evaluated. Finally, experimental results are used to verify the superiority of the combined method over other individual algorithms.

Key words: Forgetting factor least squares, Lithium-ion battery, Particle filter, State-of-charge, Unscented Kalman filter

I. INTRODUCTION

Lithium-ion batteries with high energy and power density are widely used in many applications, such as in electric vehicles (EVs) and energy storage systems. Battery state-of-charge (SOC) estimation plays an essential role in battery management systems to ensure safe and reliable operation. However, the SOC of lithium-ion batteries cannot be measured directly and has to be estimated based on measurable variables, such as voltage, current, and temperature.

Existing theses have proposed many SOC estimation algorithms, including the ampere–hour integral method [1], [2], the open-circuit voltage (OCV) method [3], [4], the Kalman filter (KF) algorithm [5], the extended KF (EKF) algorithm [6]-[8], the unscented KF (UKF) algorithm [9], the neural network algorithm [10], and the fuzzy algorithm [11]. The ampere–hour integral method is simple and easy to implement; it is widely used in battery management chips [12]. The OCV method requires a long standing time, and thus, it is unsuitable for online measurement and estimation. The KF algorithm is a closed-loop algorithm that can gradually modify estimation results through iterations. However, a lithium-ion battery is a nonlinear system; hence, KF estimation generates an evident error. The EKF algorithm uses a first-order Taylor series to transform a nonlinear system into a linear system. However, if the nonlinear system is a high-order system, then a large error will be produced. Meanwhile, the accuracy of the EKF algorithm depends on model parameters. The neural network algorithm is a type of machine learning language that can be applied to simulate the complex dynamic characteristics of a battery and estimate its SOC. However, the performance of this algorithm depends on model training data and methods. Furthermore, the computational complexity of this method is high and its learning time is extremely long. Thus, the neural network algorithm is unsuitable for online estimation. The UKF algorithm introduces unscented transformation (UT) to nonlinear estimation. Although the accuracy of UKF is high, it is characterized by slow convergence and poor robustness.

Other improved algorithms have been proposed in recent years, such as the dual EKF (DEKF) [13], the iterated EKF (IEKF) [14], the strong tracking KF (STKF) [15], the square root UKF (SRUKF) [16], and the sliding mode observer [17]. In [13], DEKF provided a bootstrapping procedure for combined state and parameter estimation using two parallel EKFs. This method improves the accuracy of SOC estimation. In [14], IEKF was used to enhance accuracy. Reference [15]

Manuscript received May 18, 2017; accepted Aug. 27, 2017
Recommended for publication by Associate Editor Jonghoon Kim.
†Corresponding Author: lgdtju@tju.edu.cn
Tel: +82-27890983, Fax: +86-22-27406705, Tianjin University
*School of Electrical and Information Eng., Tianjin University, China

showed that STKF provides a more accurate SOC estimation than EKF; STKF also exhibits the advantages of tracking variables and adjusting error covariance online. Reference [16] proposed a new SOC estimation method based on SRUKF using spherical transform (Sqrt-UKFST) with a unit hyper sphere; this method achieves a lower error than EKF. Reference [17] proposed a novel sliding mode observer SOC estimation algorithm with improved accuracy and robustness. Reference [18] compared the merits and demerits of EKF and UKF in terms of convergence rate and estimation accuracy based on the existing literature. A conclusion was drawn that UKF is considerably better, with faster convergence and higher accuracy than EKF.

In recent years, the PF algorithm has gradually attracted the attention of researchers and has been applied to the SOC estimation of lithium-ion batteries [18], [19]. The PF algorithm can solve the nonlinear non-Gaussian estimation problem and requires less iteration to converge with high accuracy. However, its computational complexity is high.

These improved algorithms mainly focus on one performance aspect and have respective merits and demerits. In the current study, the forgetting factor least squares (FFLS) algorithm is used to identify the model parameters of lithium-ion batteries online. Then, the combination of the UKF and PF algorithms is applied to implement an online SOC estimation with high accuracy and low runtime. The PF algorithm is adopted to decrease estimation error, whereas the UKF algorithm is used to obtain actual SOC with short iteration time. The experimental results verify the validity of the combined method.

The remainder of this paper is organized as follows. Section II introduces the battery model and online parameter identification. Section III presents the UKF and PF algorithms and then proposes the switch strategy for the combination. In Section IV, the superiority of the combined method is verified using the experimental data. The estimation results of EKF, UKF, PF, and the combined method are compared. The conclusion is presented in Section V.

II. Battery Model

A. Model Structure

The lithium-ion battery model plays a pivotal role in ensuring the accuracy and complexity of SOC estimation; this model is mainly classified as an electrochemical, electrical, or mathematical model [20]–[22]. The combined electrochemical model is based on three first-order simple electrochemical models and can accurately describe the internal electrochemical reaction of lithium-ion batteries [6], [28].

Then, the state equation of the lithium-ion battery combined model is expressed as

$$\mathrm{SOC}(t) = \mathrm{SOC}(0) + \int_0^t \frac{\eta i(t)}{Q_c} dt \,, \tag{1}$$

where $SOC(t)$ is the SOC value at time t; $SOC(0)$ is the initial value; $i(t)$ is the current at time t, charging is positive and discharging is negative; η is the energy conversion efficiency, which is set to 1; and Qc is the electric charge of the lithium-ion battery.

The measurement equation of the lithium-ion battery combined model is expressed as

$$\begin{aligned} U(t) = K_0 - K_1 SOC(t) + \frac{K_2}{SOC(t)} + K_3 \ln(SOC(t)) \\ + K_4 \ln(1 - SOC(t)) - R_0 i(t) \end{aligned} \,, \tag{2}$$

where $U(t)$ is the terminal voltage at time t; K_0, K_1, K_2, K_3, and K_4 are the identified parameters; and R_0 is the internal resistance of the lithium-ion battery.

B. Model Parameter Identification

The parameters of the battery model are closely related to the electrochemical reaction and are affected by the temperature and the depth of charge and discharge [27]. The accuracies of the voltage and current sensors also affect the identification of the combined model [19], [23]. Conventional off-line identification algorithms cannot accurately follow the variations of battery parameters [24]; thus, FFLS is used in this study to identify the battery model online. FFLS eliminates data saturation and accurately reflects system characteristics by assigning different weights to new and old data. In addition, FFLS exhibits the advantages of rapid convergence and powerful tracking capability [25].

The measurement equation, i.e., Eq. (2), is rewritten as follows:

$$U(t) = C(t)X(t) \,, \tag{3}$$

where

$$C(t) = [1, -SOC(t), \frac{1}{SOC(t)}, \ln(SOC(t)), \ln(1 - SOC(t)), -i(t)] \,, \tag{4}$$

$$X(t) = [K_0, K_1, K_2, K_3, K_4]^T \,. \tag{5}$$

Then, the sampling period T, $SOC(0)$, $U(0)$, estimated parameter $X(0)$, and covariance matrix $P(0)$ are initialized.

From the estimated value $X(t-1)$ of time $t-1$, the estimated value $X(t)$ at time t is calculated as

$$X(t) = X(t-1) + K(t)[U(t) - C(t)X(t-1)] \,, \tag{6}$$

where $U(t)$ is the measured voltage.

Gain $K(t)$ and covariance matrix $P(t)$ are calculated as

$$K(t) = P(t-1)C(t)\left[\lambda + C^T(t)P(t-1)C(t)\right]^{-1} \,, \tag{7}$$

$$P(t) = \frac{1}{\lambda}\left[I - K(t)C^T(t)\right]P(t-1) \,, \tag{8}$$

where $C^T(t)$ is the transposition of $C(t)$; and λ is the forgetting factor, which is set to a value between 0.95 and 1.

In this manner, the electrochemical model parameters can be identified using an iteration process.

C. Battery Modeling Results

A LiFePO4 cell, which has a nominal capacity of 12.5 Ah, is

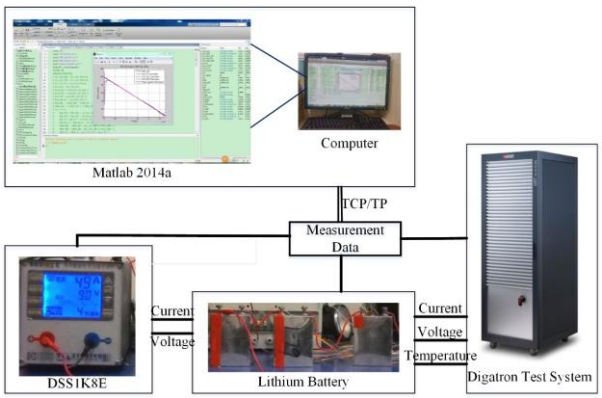

Fig. 1. Test platform of lithium-ion battery.

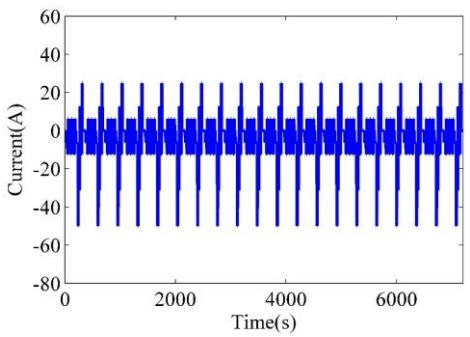

Fig. 2. DST current profile.

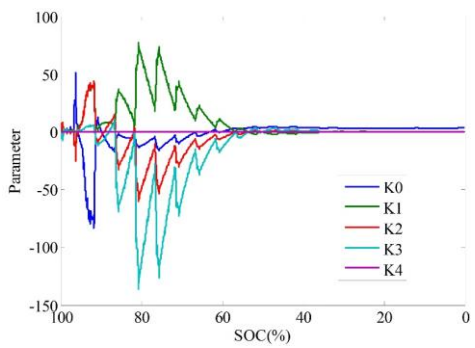

Fig. 3. Identified parameters.

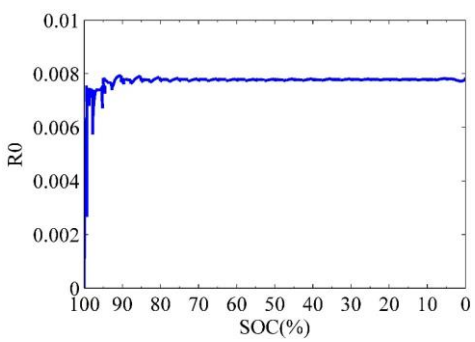

Fig. 4. Identified R_0.

used in the experiment. The battery test platform, which includes the Digatron battery testing system, a DSS1K8E programmable electronic load, and a USB2812 data acquisition card, is shown in Fig. 1.

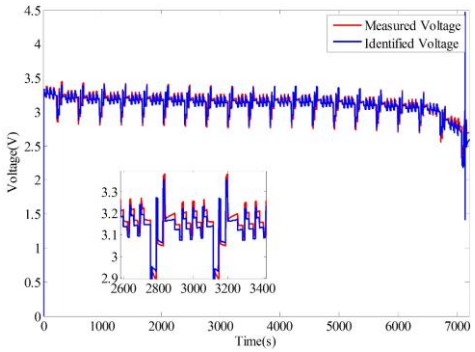

Fig. 5. Measured and identified voltages.

The USB2812 data acquisition card is used to collect lithium-ion battery voltage and charge and discharge currents. Then, the data are processed using MATLAB 2014a software. The configuration of the computer is Intel® Core™ 2 Duo E7500, with a memory of 4 GB, and a 64-bit operating system.

In this study, the dynamical stress testing (DST) profile is used for online parameter identification [26]. During the experiment, the sampling periods of voltage and current are set to 1 s, and the DST current profile is shown in Fig. 2.

The initial SOC of the battery is set to 100%, and the identification results of K_0, K_1, K_2, K_3, and K_4 based on FFLS are presented in Fig. 3. Meanwhile, the internal resistance (R_0), which is approximately 0.008 Ω, is shown in Fig. 4.

The terminal voltage continuously decreases to the discharge cutoff voltage in the DST test. The battery voltages from the FFLS algorithm and the experimental measurement are shown in Fig. 5. The high accuracy and the small root-mean-square error (RMSE) of the voltage (approximately 0.0661 V) prove that the estimated combined model can effectively simulate the charge and discharge characteristics of lithium-ion batteries.

III. SOC Estimation Process

A battery exhibits a self-discharge effect, and thus, the remaining energy is unknown when a battery is replaced or stored for a long time. Consequently, the initial estimation error of battery SOC is high. A combined method is adopted in this study by considering the particular merits of UKF and PF. Rapid convergence and high accuracy are achieved through a switch between UKF and PF.

A. UKF Algorithm

UKF is a new type of estimation algorithm. In contrast to the linearization function of EKF, UKF is based on UT and uses the KF algorithm framework. Several sigma points are used to calculate the mean and covariance for a prior estimation equation [9]. In general, the number of sigma points is set to $2n+1$ for a state equation in n-dimension, and the sigma points and weights are generated using Eqs. (9) and (10).

$$X_t^i = \left[\overline{X}_t \quad \overline{X}_t + \sqrt{(n+\lambda) P_t} \quad \overline{X}_t - \sqrt{(n+\lambda) P_t} \right], \tag{9}$$

$$\begin{cases} \omega_m^1 = \dfrac{\lambda}{n+\lambda} \\ \omega_c^1 = \dfrac{\lambda}{n+\lambda} + (1-\alpha^2+\beta) \\ \omega_m^i = \omega_c^i = \dfrac{\lambda}{2(n+\lambda)}, i = 2 \sim 2n+1 \end{cases}, \tag{10}$$

where P is the covariance of the state variables, and $\overline{X}$ is the mean of the state variables. ω_m^i is the weight of the mean of the i^{th} sample point, and ω_c^i is the weight of the i^{th} sample point variance. λ is a scaling parameter used to reduce the total estimation error; it can be calculated as $\lambda = \alpha^2(n+\kappa) - n$.

Then, the one-step estimation values of the state and covariance matrices are calculated for each sigma point as follows:

$$\begin{cases} \overline{X_{t+1}^i} = \sum_{i=1}^{2n+1} \omega_m^i f(X_t^i, U_{t+1}) \\ P_x = \sum_{i=1}^{2n+1} \omega_c^i (X_{t+1}^i - \overline{X_{t+1}^i})(X_{t+1}^i - \overline{X_{t+1}^i})^T + Q \end{cases}. \tag{11}$$

The estimated measurement and covariance matrices are calculated as

$$\begin{cases} \overline{Z_{t+1}^i} = \sum_{i=1}^{2n+1} \omega_m^i h(X_{t+1}^i, U_{t+1}), i = 1 \sim 2n+1 \\ P_z = \sum_{i=1}^{2n+1} \omega_c^i (Z_{t+1}^i - \overline{Z_{t+1}^i})(Z_{t+1}^i - \overline{Z_{t+1}^i})^T + R \end{cases}. \tag{12}$$

The Kalman gain and cross-covariance are expressed as

$$\begin{cases} P_{xz} = \sum_{i=1}^{2n+1} \omega_c^i (X_{t+1}^i - \overline{X_{t+1}^i})(Z_{t+1}^i - \overline{Z_{t+1}^i})^T \\ K_{t+1} = P_{xz} P_z^{-1} \end{cases}. \tag{13}$$

The state estimation and error covariance are updated using Eq. (14) as follows:

$$\begin{cases} X_{t+1} = \overline{X_{t+1}^i} + K_{t+1}(U_{t+1} - \overline{Z_{t+1}^i}) \\ P_{t+1} = P_t - K_{t+1} P_t K_{t+1}^T \end{cases}. \tag{14}$$

B. PF Algorithm

PF uses nonparametric Monte Carlo simulation and posteriori filtering to realize recursive Bayesian filtering. This algorithm can be applied to any nonlinear system described by the state space model and provides an effective solution [18].

To solve the difficulty caused by integral calculation in the Bayesian posterior, Monte Carlo sampling is used to calculate a posteriori probability. Different particle weights are relevant to their individual confidence, and all state values are weighted as sums of the particles as follows:

$$p(X_{0:t} \mid U_{1:t}) \approx \sum_{i=1}^{N_s} \omega_t^i \delta(X_{0:t} - X_{0:t}^i). \tag{15}$$

The normalized weights can be calculated as

$$\omega_t^i = \omega_{t-1}^i \frac{p(Z_t \mid X_t^i) p(X_t^i \mid X_{t-1}^i)}{q(X_t \mid X_{0:t-1}^i, Z_{1:t})}. \tag{16}$$

The estimation of a posteriori filtering probability requires all measured data, and new measurement is necessary to recalculate the weights of the entire sequence of states. The sequential importance sampling and resampling method is used to recursively calculate the weights.

The first step in SOC estimation involves calculating the state prior estimation for particles that use state Eq. (1). Then, the weights are calculated using Eqs. (15) and (16). SOC state and voltage estimation can be updated.

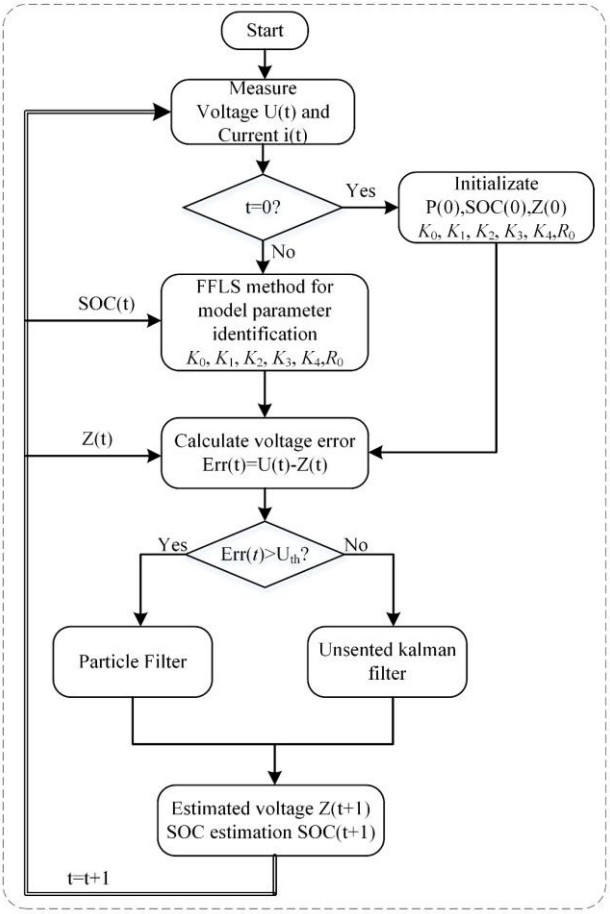

Fig. 6. Flowchart of the combined method for SOC estimation.

$$X_{t+1} = \sum_{i=1}^{N_s} \omega_t^i X_t^i, \tag{17}$$

$$Z_{t+1} = \sum_{i=1}^{N_s} \omega_t^i Z_t^i. \tag{18}$$

After state estimation and measurement, the weights of the particles should be normalized as

$$\omega_t^i = \frac{\omega_t^i}{\sum_{i=1}^{N_s} \omega_t^i}. \tag{19}$$

To prevent particle degeneration, low-weight particles are removed, whereas high-weight particles are retained. Then, a new set of particles $\{X_{0:t}^i\}_{i=1}^{N_s}$ is obtained.

C. Criterion for Algorithm Switch

The process of the SOC estimation method is described as follows.

Step 1: Initialization and data measurement

System noise (Q), measurement noise (R), the covariance matrix (P) and the battery nominal charge quantity (Q_c) of the lithium-ion battery, and the threshold value (U^{th}) of

voltage error are set. The current and voltage of the lithium-ion battery are obtained from the Federal Urban Driving Schedule (FUDS) loading profiles.

Step 2: For t = 1, 2, 3, …, N

(a) With $SOC(t)$ and current $i(t)$ at time t, parameters K_0, K_1, K_2, K_3, K_4, and R_0 are identified by the FFLS algorithm. The state and measurement equations are updated with the identified parameters.

(b) The voltage error is calculated according to the measured voltage and the estimated voltage.

$$Er(t)=|U(t)-Z(t)|, \quad (20)$$

where $U(t)$ is the measured voltage at time t, and $Z(t)$ is the estimated voltage using the PF or UKF algorithm.

(c) The combined algorithm is used to estimate the SOC of lithium-ion battery with the parameters at time t. When $Err(t)$ is higher than U^{th}, PF is used; otherwise, UKF is used.

(d) For the next operating time step t+1, the process in (a) is repeated.

The flowchart of the combined method for SOC estimation is shown in Fig. 6.

In the combined method, FFLS provides an accurate battery model that is beneficial for SOC estimation. When voltage error exceeds the threshold, the PF algorithm is used to decrease convergence time. Otherwise, the UKF algorithm is applied to reduce computational complexity.

IV. Experimental Results

A. Experimental Setup

In the experiment, the lithium-ion battery is controlled under the FUDS test to simulate its actual working condition. The measured current profile of FUDS is shown in Fig. 7(a). The discharge capacity of each FUDS test cycle is 5% of the total capacity. Therefore, battery voltage discharges from full charge (3.65 V) to the cutoff voltage (2.8 V) after 20 test cycles. The profile of the discharge current is shown in Fig. 7(b), and the profile of the measured voltage is presented in Fig. 7(c). The SOC value calculated using the integration method is shown in Fig. 7(d). This value will be adopted as the actual value in the subsequent estimation.

B. Choice of Particle Number

The accuracy and computational complexity of the PF algorithm depend on the number of sampling particles N_s. The estimation error and runtime under different values of N_s are presented in Fig. 8. The figure shows that when N_s > 100, PF estimation error does not change evidently. However, a high computational complexity is induced. Hence, to simultaneously achieve high accuracy and low computational complexity, N_s = 100 is selected in this study.

In the experiment, the combined method is used to estimate the voltage of the lithium-ion battery based on the FUDS

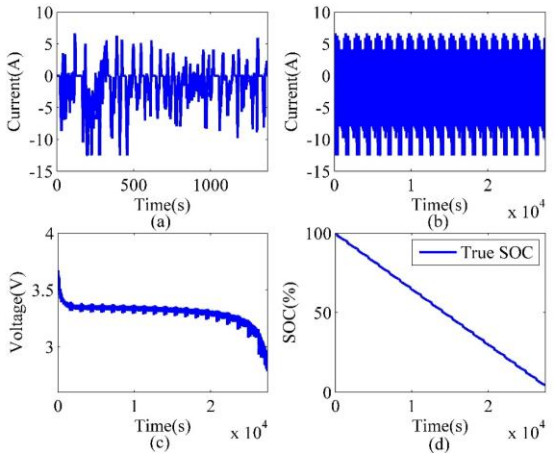

Fig. 7. (a) Current of FUDS test, (b) measured current, (c) measured voltage, and (d) true SOC.

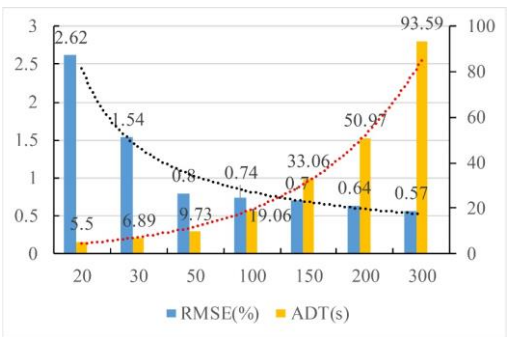

Fig. 8. Estimation error and runtime under different values of N_s.

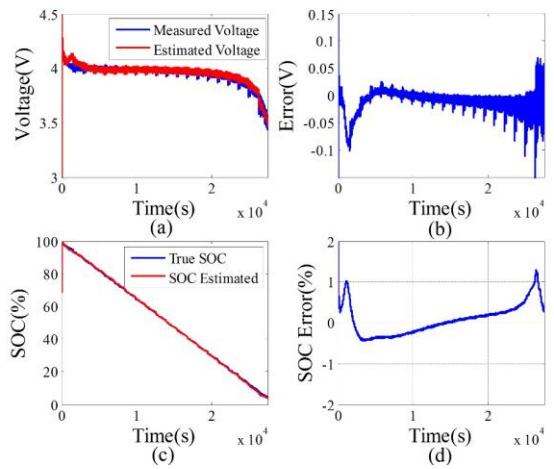

Fig. 9. (a) Voltage, (b) voltage error, (c) SOC with an initial value of 100%, and (d) SOC error.

discharge curve. First, the initial SOC value is set to the true value. The estimated voltage and voltage error curves are presented in Figs. 9(a) and 9(b). These figures show that the estimated voltage matches the actual value. The maximum voltage error is approximately 0.15 V, and RMSE can be calculated as 0.0289 V. Meanwhile, the estimated SOC and estimation error are shown in Figs. 9(c) and 9(d), where the estimated SOC can also fit the actual SOC variation. The SOC

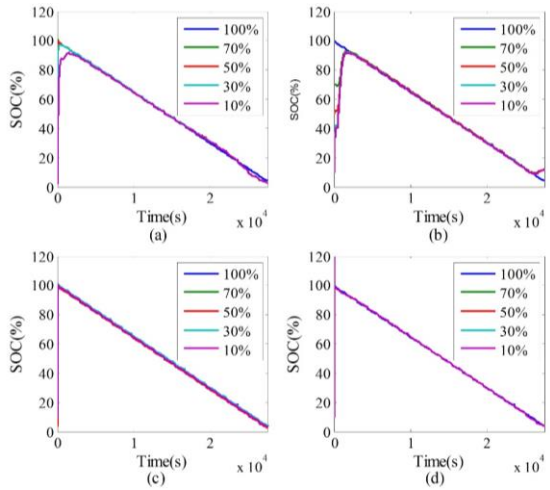

Fig. 10. SOC estimation under different initial values. (a) EKF, (b) UKF, (c) PF, (d) the proposed algorithm.

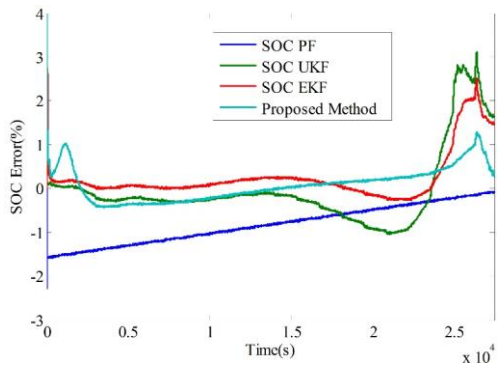

Fig. 11. Comparison of SOC errors with an initial value of 100%.

error can be maintained within 2.5%, the calculated mean error is 0.31%, and RMSE is 0.0074 V. These results prove that the combined method exhibits high estimation accuracy for a small initial SOC error.

Various SOC estimation algorithms provide varying performances under different initial SOC values. Fig. 10 shows the estimation results of EKF, UKF, PF, and the combined method with initial SOC values of 70%, 50%, 30%, and 10%, respectively.

Fig. 10 shows that the four algorithms can estimate SOC variation. However, further analysis shows that their estimation errors and convergence speeds differ.

The initial SOC value is set to the actual value, and the SOC estimation errors of the four algorithms are presented in Fig. 11. The SOC estimation of the combined method achieves the highest accuracy.

To fully analyze the performance of the different algorithms, the mean absolute error (MAE), RMSE, and the average execution time (AET) of the estimated SOC from the four algorithms are compared as shown in Fig. 12. Compared with EKF, UKF, and PF, the combined method provides the most accurate estimated results. Although the RMSE of PF is less than those of the other algorithms, which indicates that the

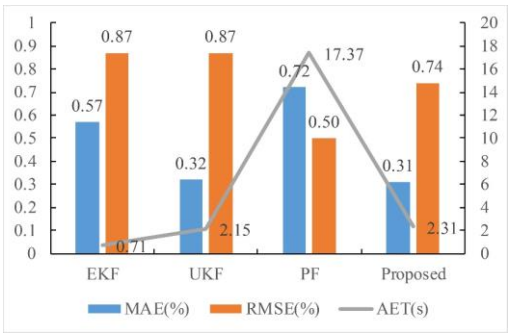

Fig. 12. Performance comparison of the four algorithms.

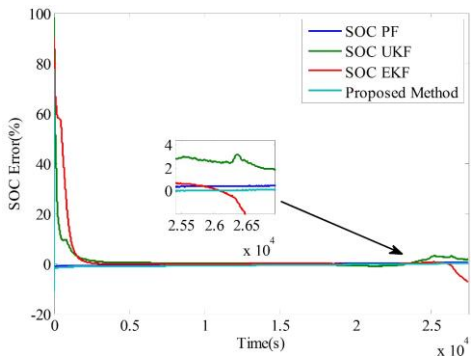

Fig. 13. Comparison of SOC errors with an initial value of 10%.

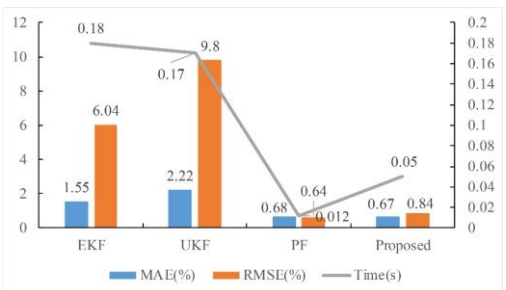

Fig. 14. Comparison of algorithm convergence.

estimated results of PF are more stable, the AET of PF (17.37 s) is considerably longer than those of the other algorithms.

The initial SOC is set to 10%, and the estimated SOC errors from EKF, UKF, PF, and the combined method are shown in Figs. 13 and 14. Acceptable results can be obtained under normal battery condition. However, the errors of EKF and UKF increase as battery parameters vary, as depicted in the small window in Fig. 13. Moreover, the comparison of Figs. 12 and 14 shows that the MAEs of EKF and UKF are more evident under 10% initial SOC than under the actual initial SOC. By contrast, PF and the combined method can limit errors within a narrower region.

Meanwhile, when the SOC value reaches the average level, it is referred to as estimation convergence. Then, the convergence time can be compared and summarized in Fig. 14. The figure shows that the convergence time of the combined method is shorter than those of UKF and EKF, but slightly

longer than that of PF. However, given that AET is not dependent on the initial SOC, PF will require longer runtime for the entire process as shown in Fig. 12. Therefore, the combined method provides a more balanced performance than the other algorithms.

V. CONCLUSIONS

A combined method for the SOC estimation of lithium-ion batteries is proposed in this study. This method combines the advantages of the PF and UKF algorithms. To improve the accuracy of the battery model, the FFLS algorithm is used to identify model parameters. A small RMSE of voltage is obtained (approximately 0.0661 V). Then, the switch criterion for PF and UKF is proposed. This criterion is based on the measured and estimated voltages of the battery. Compared with the individual EKF, UKF, and PF algorithms, the combined method provides a good trade-off among MAE, RMSE, and AET. Hence, the combined method will be beneficial for a real-time and accurate battery management system.

REFERENCES

[1] S. N. Kong, C.-S. Moo, Y.-P. Chen, and Y.-C. Hsieh, "Enhanced coulomb counting method for estimating state-of-charge and state-of-health of lithium-ion batteries," *Applied Energy*, Vol. 86, No. 9, pp. 1506-1511, Sep. 2009.

[2] N. Yang and G. Li, "State of charge estimation for pulse discharge of a LiFePO4 battery by a revised Ah counting," *Electrochim Acta*, Vol. 151, No. 1, pp. 63-71, Jan. 2015.

[3] S. Lee, J. Kim, J. Lee, and B. H. Cho, "State-of-charge and capacity estimation of lithium-ion battery using a new open-circuit voltage versus state-of-charge," *Journal of Power Sources*, Vol. 185, No. 2, pp. 1367-1373, Dec. 2008.

[4] N. A. Windarko and J. Choi, "SOC estimation based on OCV for NiMH batteries using an improved takacs model," *J. Power Electron.*, Vol. 10, No. 2, pp.181-186, Mar. 2010.

[5] P. Spagnol, S. Rossi, and S. M. Savaresi, "Kalman filter SoC estimation for Li-Ion batteries," *in 2011 IEEE International Conference on Control Applications (CCA)*, pp. 587-592, Sep. 2011.

[6] G. L. Plett, "Extended Kalman filtering for battery management systems of LiPB-based HEV battery packs: Part 2. modeling and identification," *J. Power Sources*, Vol. 134, No. 2, pp. 262-276, Aug. 2004.

[7] G. L. Plett, "Extended Kalman filtering for battery management systems of LiPB-based HEV battery packs: Part 3. State and parameter estimation," *Journal of Power Sources*, Vol. 134, No. 2, pp. 277-292, Aug. 2004.

[8] N. A. Windarko and J. Choi, "LiPB battery SOC estimation using extended Kalman filter improved with variation of single dominant parameter," *J. Power Electron.*, Vol. 12, No. 1, pp.40-48, Jan. 2012.

[9] G. L. Plett, "Sigma-point Kalman filtering for battery management systems of LiPB-based HEV battery packs: Part 1: Introduction and state estimation," *J. Power Sources*, Vol. 161, No. 2, pp. 1356-1368, Oct. 2006.

[10] W. He, N. Williard, C. Chen, and M. Pecht, "State of charge estimation for Li-ion batteries using neural network modeling and unscented Kalman filter-based error cancellation," *International Journal of Electrical Power & Energy Systems*, Vol. 62, No. 11, pp. 783-791, Nov. 2014.

[11] X. Chen, W. Shen, Z. Cao, A. Kapoor, and I. Hijazin, "Adaptive gain sliding mode observer for state of charge estimation based on combined battery equivalent circuit model," *Computers & Chemical Engineering*, Vol. 64, No. 18, pp. 114-123, Jun. 2014.

[12] F. Yang, Y. Xing, D. Wang, and K.-L. Tsui, "A comparative study of three model-based algorithms for estimating state-of-charge of lithium-ion batteries under a new combined dynamic loading profile," *Applied Energy*, Vol. 164, pp. 387-399, Feb. 2016.

[13] J. Kim, S. Lee, and B. H. Cho, "Complementary cooperation algorithm based on DEKF combined with pattern recognition for SOC/Capacity estimation and SOH estimation," *IEEE Trans. Power Electron.*, Vol. 27, No. 1, pp. 436-451, Jan. 2012.

[14] S. Sepasi, R. Ghorbani, and B. Y. Liaw, "Improved extended Kalman filter for state of charge estimation of battery pack," *J. Power Sources*, Vol. 255, No. 1, pp. 368-376, Jun. 2014.

[15] D. Li, J. Ouyang, H. Li, and J. Wan, "State of charge estimation for LiMn2O4, power battery based on strong tracking sigma point Kalman filter," *J. Power Sources*, Vol. 279, pp. 439-449, Apr. 2015.

[16] H. Gholizade-Narm and M. Charkhgard, "Lithium-ion battery state of charge estimation based on square-root unscented Kalman filter," *IET Power Electronics*, Vol. 6, No. 9, pp. 1833-1841, Nov. 2013.

[17] Q. Chen, J. Jiang, S. Liu, and C. Zhang, "A novel sliding mode observer for state of charge estimation of EV lithium batteries," *J. Power Electron.*, Vol. 16, No. 3, pp.1131-1140, May. 2016.

[18] M. Gao, Y. Liu, and Z. He, "Battery state of charge online estimation based on particle filter," in *Image and Signal Processing (CISP), 2011 4th International Congress* pp. 15-17, 2011.

[19] X. Liu, Z. Chen, C. Zhang, and J. Wu, "A novel temperature-compensated model for power Li-ion batteries with dual-particle-filter state of charge estimation," *Applied Energy*, Vol. 123, pp. 263-272, Jun. 2014.

[20] L. Zheng, L. Zhang, J. Zhu, G. Wang, and J. Jiang, "Co-estimation of state-of-charge, capacity and resistance for lithium-ion batteries based on a high-fidelity electrochemical model," *Applied Energy*, Vol. 180, pp. 424-434, Oct. 2016.

[21] C. Lin, H. Mu, R. Xiong, and W. Shen, "A novel multi-model probability battery state of charge estimation approach for electric vehicles using H-infinity algorithm," *Applied Energy*, Vol. 166, pp. 76-83, Mar. 2016.

[22] H. He, R. Xiong, H. Guo, and S. Li, "Comparison study on the battery models used for the energy management of batteries in electric vehicles," *Energy Conversion and Management*, Vol. 64, pp. 113-121, Dec. 2012.

[23] Y. He, X. T. Liu, C. B. Zhang, and Z. H. Chen, "A new model for State-of-Charge (SOC) estimation for high-power Li-ion batteries," *Applied Energy*, Vol. 101, No. 1, pp. 808-814, Jan. 2013.

[24] H. Rahimi-Eichi, F. Baronti, and M. Y. Chow, "Online adaptive parameter identification and state-of-charge coestimation for lithium-ion-polymer battery cells," *IEEE Trans. Ind. Electron.*, Vol. 61, No. 4, pp. 2053-2061, Apr. 2014.

[25] D. Zhou, A. Ravey, F. Gao, A. Miraoui, and K. Zhang, "On-line estimation of lithium polymer batteries state-of-charge using particle filter based data fusion with multi-models approach," *Industry Applications Society*

Meeting. IEEE, pp. 1-8, 2015.
[26] *USABC electric vehicle Battery Test Procedures Manual. Revision 2*, DOE/ID-10479, 1996.
[27] J. Kim, S. Lee, and B. Cho, "Discharging/charging voltage-temperature pattern recognition for improved SOC/ capacity estimation and SOH prediction at various temperatures," *J. Power Electron.*, Vol. 12, No. 1, pp. 1-9, Jan. 2012.
[28] C. Zou, C. Manzie, D. Nesic, A. G. Kallapur, "Multi-time-scale observer design for state-of-charge and state-of-health of a lithium-ion battery," *J. Power Sources*, Vol. 335, pp. 121-130, Oct. 2016.

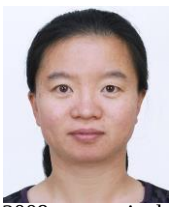

Guidan Li was born in China in 1975. After obtaining her B.S. from Tianjin University (TJU), China, in 1998, she worked as a teaching assistant in the School of Electrical Engineering and Automation of TJU. While working, she obtained her M.S. and Ph.D. in Electrical Engineering from TJU in 2004 and 2009, respectively. She was a lecturer from 2006 to 2010. She has been an associate professor since 2010. She was a visiting scholar at the University of Central Florida, USA from March 2014 to March 2015. Her main research interests include power electronic techniques and their applications.

Kai Peng was born in China in 1994. He obtained his B.S. in Microelectronics from Tianjin University (TJU), China in 2015. He is currently working on an M.S. in Electrical Engineering at TJU. His research interests include power batteries of electric vehicles and battery management systems.

Bin Li was born in China in 1976. He obtained his Ph.D. in Electrical Engineering from Tianjin University (TJU), Tianjin, China in 2006. He was a lecturer in the School of Electrical Engineering and Automation of TJU from 2004 to 2009. He has been an associate professor at TJU since 2009. He was a visiting scholar at the Department of Electrical Engineering and Computer Science of the University of Central Florida in Orlando, Florida, USA from March 2014 to March 2015. His current research interests include electric machine design and control.